

Exactly solvable quantum impurity model with inverse-square interactions

Hong-Hao Tu^{1,*} and Ying-Hai Wu^{2,†}

¹*Institut für Theoretische Physik, Technische Universität Dresden, 01062 Dresden, Germany*

²*School of Physics and Wuhan National High Magnetic Field Center, Huazhong University of Science and Technology, Wuhan 430074, China*

We construct an exactly solvable quantum impurity model which consists of spin-1/2 conduction fermions and the spin-1/2 magnetic moment. The ground state is a Gutzwiller projected Fermi sea with non-orthonormal modes and its wave function in the site-occupation basis is a Jastrow-type homogeneous polynomial. The parent Hamiltonian has all-to-all inverse-square hopping terms between the conduction fermions and inverse-square spin-exchange terms between the conduction fermions and the magnetic moments. The low-lying energy levels, spin-spin correlation function, and von Neumann entanglement entropy of our model demonstrate that it exhibits the essential aspects of spin-1/2 Kondo physics. The machinery developed in this work can generate many other exactly solvable quantum impurity models.

Introduction — The interplay between the localized degree of freedom and itinerant electrons has been a central subject of condensed matter physics in the past decades [1, 2]. The localized degree of freedom is usually called impurity and the simplest example is spin-1/2 magnetic moments due to unpaired d or f electrons in solids. The unpaired electron is screened by the itinerant electrons via spin-exchange interactions at low temperatures and a spin-singlet state emerges. Quantum impurity physics has also been investigated in quantum dots [3, 4], magnetic adatoms on metallic surfaces [5], carbon nanotubes [6, 7], and quantum Hall devices [8–10]. The impurity may even be realized in a non-local manner using Majorana zero modes in topological superconductors [11–16].

The theoretical understanding of quantum impurity physics begins with two models proposed by Anderson and Kondo, which are related by the Schrieffer-Wolff transformation [17–19]. To explain a mysterious change of resistance in certain metallic samples with dilute magnetic atoms, Kondo constructed a model with one magnetic moment coupled to a bath of conduction electrons via a spin-exchange term. The simplicity of this model is highly deceptive as manifested by divergences in straightforward perturbative calculations, which calls for drastically different approaches. Based on the idea of renormalization, Wilson developed the numerical renormalization group (NRG) method and brought out a rather complete solution of the Kondo problem [20–22]. The Kondo problem elucidates the concept of asymptotic freedom and serves as a vivid demonstration of correlation effects in many-body systems.

Further insights into the Kondo physics were gathered along several directions. The NRG results helped Nozières to formulate a Fermi liquid theory for the low-energy physics of the spin-1/2 Kondo model [23]. The magnetic moment is only coupled to one particular mode of the conduction fermions and other modes in the conduction bath remain free. Affleck and Ludwig applied boundary conformal field theory (CFT) to study Kondo

physics [24, 25]. This approach reconstructs the Fermi liquid picture for the spin-1/2 Kondo model, but its utility extends to more complicated quantum impurity systems that are not amenable to the Fermi liquid description. Andrei and Wiegmann independently constructed a Kondo model which can be solved exactly using the Bethe ansatz [26–29]. It is defined on a semi-infinite continuous chain populated by fermions with linear dispersion relation. The Kondo physics has also been explored in some other exactly solvable models [30–34].

In this Letter, we propose an exactly solvable quantum impurity model in a one-dimensional open chain with spin-1/2 conduction fermions and one spin-1/2 magnetic moment at one end of the chain. This model is very different from the one by Andrei and Wiegmann: it can be defined on any finite-size lattices; the conduction fermions have a quadratic dispersion relation in a special basis; the lowest eigenstates in all cases with an odd number of conduction fermions are known. The low-lying energy levels, entanglement entropy, and spin-spin correlation function of our model clearly demonstrate that it exhibits spin-1/2 Kondo physics. It is further suggested that our model may be non-integrable based on the level statistics of the full energy spectrum.

The most appealing property of our model is the existence of highly structured eigenstates that can be expressed in three different but equivalent ways: Gutzwiller projected Fermi seas with non-orthogonal basis states, Jastrow-type homogeneous polynomial wave functions, correlators of the CFT for the system. The Gutzwiller approach elucidates Nozières’ Fermi liquid picture in an analytically tractable manner. The CFT approach is reminiscent of the well-established connection between edge CFT and bulk wave function in quantum Hall systems [35]. The machinery developed in this work opens up the exciting possibility of constructing a variety of exactly solvable quantum impurity models.

Wave function — The system of our interest is an open chain with $L + 1$ sites (L can be even or odd) labeled by $j = 0, 1, \dots, L$ [Fig. 1(a)]. It is placed on the semi-circle

with unity radius and projected onto the real line $[-1, 1]$. The angular position of the j -th site is $\theta_j = \frac{\pi}{L}(j - 1/2)$ for $1 \leq j \leq L$ and $\theta_j = 0$ for $j = 0$, and the associated linear position is $u_j = \cos \theta_j$. The motivation for this choice of coordinate will become clear later. The $1 \leq j \leq L$ sites are populated by spin-1/2 conduction fermions described by creation (annihilation) operators $c_{j,\sigma}^\dagger$ ($c_{j,\sigma}$) with $\sigma = \uparrow, \downarrow$ being the spin index. The $j = 0$ site is occupied by a spin-1/2 magnetic moment described by operators \mathbf{S}_0 . The magnetic moment can be represented using Abrikosov fermions as $\mathbf{S}_0 = \frac{1}{2} \sum_{\sigma\sigma'} c_{0,\sigma}^\dagger \vec{\tau}_{\sigma\sigma'} c_{0,\sigma'}$ with $\vec{\tau}$ being the Pauli matrices [2]. The redundancy caused by this representation is removed by imposing the single-occupancy constraint $\sum_{\sigma} c_{0,\sigma}^\dagger c_{0,\sigma} = 1$.

The many-body state to be investigated is

$$|\Psi\rangle = \sum_{\{n_j^\uparrow\}, \{n_j^\downarrow\}} \Psi(\{n_j^\uparrow\}, \{n_j^\downarrow\}) (c_{0,\uparrow}^\dagger)^{n_0^\uparrow} \dots (c_{L,\uparrow}^\dagger)^{n_L^\uparrow} \times (c_{0,\downarrow}^\dagger)^{n_0^\downarrow} \dots (c_{L,\downarrow}^\dagger)^{n_L^\downarrow} |0\rangle. \quad (1)$$

The coefficient

$$\Psi(\{n_j^\uparrow\}, \{n_j^\downarrow\}) = \delta_{n_0=1} \delta_{\sum_j n_j^\uparrow = \sum_j n_j^\downarrow = M} \times \prod_{\sigma=\uparrow,\downarrow} \prod_{0 \leq j < k \leq L} (u_j - u_k)^{n_j^\sigma n_k^\sigma} \quad (2)$$

is the wave function in the site-occupation basis, where $n_j^\sigma = 0, 1$ is the number of fermions with spin σ at site j , $n_j = \sum_{\sigma} n_j^\sigma$ is the total number of fermions on site j , the first δ is the single-occupancy constraint required by the magnetic moment, and the second δ means that the total number of fermions (conduction plus Abrikosov fermions) with either spin is M .

The target state can be rewritten as a Gutzwiller projected Fermi sea (up to a sign factor) $|\Psi\rangle = P_0^G \prod_{m=0}^{M-1} \prod_{\sigma=\uparrow,\downarrow} \eta_{m,\sigma}^\dagger |0\rangle$, where P_0^G enforces the single-occupancy constraint and $\eta_{m,\sigma} = \sum_{j=0}^L \cos^m \theta_j c_{j,\sigma}$ [36] are non-orthogonal unnormalized orbitals constructed from linear combinations of the conduction and Abrikosov fermions [37]. The participation of the Abrikosov fermions in the Fermi sea indicates hybridization between the magnetic moment and the conduction fermions. This second quantized form makes it transparent that $|\Psi\rangle$ is a spin singlet. Gutzwiller projected states have been used extensively in strongly correlated systems [38, 39], and parent Hamiltonians were constructed for some states with an invertible Gutzwiller projector [40, 41]. This is not the case for our model so the previous method cannot be applied directly.

If we introduce another set of operators $\zeta_{0,\sigma} = \sum_{j=1}^L c_{j,\sigma}$ and $\zeta_{m,\sigma} = \sum_{j=1}^L \cos^{m-1} \theta_j (1 - \cos \theta_j) c_{j,\sigma}$ ($m \geq 1$), the target state can be simplified to [37]

$$|\Psi\rangle = \left(c_{0,\uparrow}^\dagger \zeta_{0,\downarrow}^\dagger - c_{0,\downarrow}^\dagger \zeta_{0,\uparrow}^\dagger \right) \prod_{m=1}^{M-1} \prod_{\sigma=\uparrow,\downarrow} \zeta_{m,\sigma}^\dagger |0\rangle, \quad (3)$$

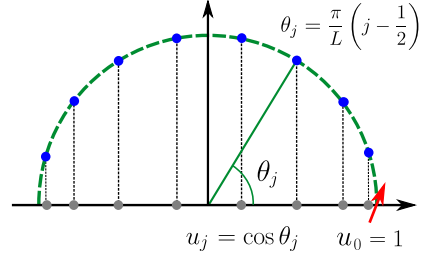


FIG. 1. Schematics of the quantum impurity model. The red arrow represents a spin-1/2 magnetic moment. The blue dots are lattice sites occupied by conduction fermions. The angular position of the j -th site is $\theta_j = \frac{\pi}{L}(j - 1/2)$ (except for $\theta_0 = 0$) and its projection on the horizontal axis is $u_j = \cos \theta_j$.

which would be of great help when one searches for the parent Hamiltonian. The Fermi liquid picture of Nozières is realized in an exact manner: the impurity forms a spin singlet with the $\zeta_{0,\sigma}^\dagger$ modes and the other conduction fermions form a Fermi sea in the non-orthogonal $\zeta_{m>0,\sigma}^\dagger$ modes. If the state with a particular M is the ground state, one can add (remove) conduction fermions to (from) the $\zeta_{m>0,\sigma}^\dagger$ modes to create excited states. However, this procedure can only give us some states in which the numbers of spin-up and spin-down fermions are equal. The Fermi liquid picture in other cases needs to be corroborated using numerical results. For the original Kondo problem, Yosida proposed a trial wave function made of a Kondo singlet and a Fermi sea of conduction fermions [42], but it does not work well [43]. The structure of Eq. (3) is very similar to the proposal of Yosida, but the crucial additional insight is that the single-particle orbitals in the Kondo singlet and the Fermi sea should be chosen properly.

Parent Hamiltonian — The target state Eq. (1) is the exact ground state of the Hamiltonian $H = \frac{\pi^2}{4L^2} (H_0 + H_P + H_K + H_C)$, where

$$H_0 = \sum_{q=0}^{L-1} \sum_{\sigma=\uparrow,\downarrow} 3q^2 d_{q,\sigma}^\dagger d_{q,\sigma} \quad (4)$$

$[d_{q,\sigma} = \sqrt{(1 + \delta_{0,q})/L} \sum_{j=1}^L \cos(q\theta_j) c_{j,\sigma}]$ describes hopping processes of the conduction fermions,

$$H_P = \frac{3}{4} \sum_{j=1}^L \sum_{\sigma=\uparrow,\downarrow} \cot^2 \theta_j c_{j,\sigma}^\dagger c_{j,\sigma} \quad (5)$$

gives site-dependent energies to the conduction fermions, and

$$H_K = \sum_{j=1}^L \cot^2 \frac{\theta_j}{2} \mathbf{S}_0 \cdot \mathbf{S}_j \quad (6)$$

stands for long-range spin-exchange interactions between the conduction fermions and the magnetic moment, and

$H_C = \sum_{j=1}^L F(L) c_{j,\sigma}^\dagger c_{j,\sigma}$ is a L -dependent chemical potential [$F(L) = -(3L^2/4 - 1)$ for odd L and $F(L) = -(3L^2/4 - 3L/2 - 1/4)$ for even L]. The real space representation of H_0 contains inverse-square hopping terms and site-dependent potential terms, as manifested by

$$H_0 = \sum_{j,k=1;j \neq k}^L \left[\frac{6(-1)^{j-k}}{|z_j - z_k|^2} - \frac{6(-1)^{j-k}}{|z_j - z_k^*|^2} \right] c_{j,\sigma}^\dagger c_{k,\sigma} + \sum_{j=1}^L \left[L^2 + \frac{1}{2} - \frac{3}{2 \sin^2 \theta_j} \right] c_{j,\sigma}^\dagger c_{j,\sigma}, \quad (7)$$

where $z_j = \exp(i\theta_j)$ and $z_j^* = \exp(-i\theta_j)$ are the complex coordinates of the site j and its mirror image with respect to the real axis [see Fig. (1)], respectively [37]. In the limit of $L \rightarrow \infty$ and $j \ll L$, the Kondo coupling strength also has an inverse-square form as $\cot^2 \frac{\theta_j}{2} \sim (j - 1/2)^{-2}$. The ratio between the largest hopping strength and Kondo coupling strength is $3/8$ as $L \rightarrow \infty$. The parent Hamiltonian has three mutually commuting conserved quantities: the total number of fermions $N_f = \sum_{j=0}^L \sum_{\sigma} c_{j,\sigma}^\dagger c_{j,\sigma}$, the total spin $\mathbf{S}^2 = (\sum_{j=0}^L \mathbf{S}_j)^2$, and its z -component $S_z = \sum_{j=0}^L S_j^z$.

It is proved in [37] that Eq. (3) is an exact eigenstate of H . The key idea is as follows. When H_K is acted on $|\Psi\rangle$, it creates particle-hole excitations (including spin-flipped ones) on top of the Fermi sea. The effect of H_P is to compensate “unwanted” particle-hole excitations created by H_K (similar to the cancellation of diffractive scattering in integrable models solved by Bethe ansatz [44]). The truly remarkable observation is that the remaining particle-hole excitations in $(H_K + H_P)|\Psi\rangle$ can be canceled completely by $H_0|\Psi\rangle$, where H_0 describes conduction fermions with a quadratic dispersion relation and discrete Chebyshev polynomials are their single-particle basis. The eigenvalue of $|\Psi\rangle$ with respect to $H_0 + H_P + H_K$ is $(M - 1)(2M^2 - M - 3/2)$. This is super-extensive (the leading term scales as M^3) so the prefactor $\pi^2/(4L^2)$ is adopted to ensure that H is physically valid. It will be demonstrated below that H_C selects the half-filled states as the ground states [$M = (L + 1)/2$ for odd L and $M = (L + 2)/2$ for even L].

Numerical results — The proof that $|\Psi\rangle$ is an eigenstate of H is not sufficient because we have claimed that it is actually the ground state. To this end, exact diagonalizations are performed for various choices of L, N_f, S_z with L up to 14. For all the cases with even N_f and $S_z = 0$, the overlaps between numerically generated lowest eigenstates and Eq. (1) are exactly 1 (up to machine precision). The half-filled states also turn out to be the ground states. The density matrix renormalization group (DMRG) [45–48] method is employed to compute the lowest eigenstates for various choices of L, N_f, S_z with L up to 80. The lowest energy of the (L, N_f, S_z) sector is denoted as $E(L, N_f, S_z)$. The accuracy of our approach can be checked by comparing numerical and analytical

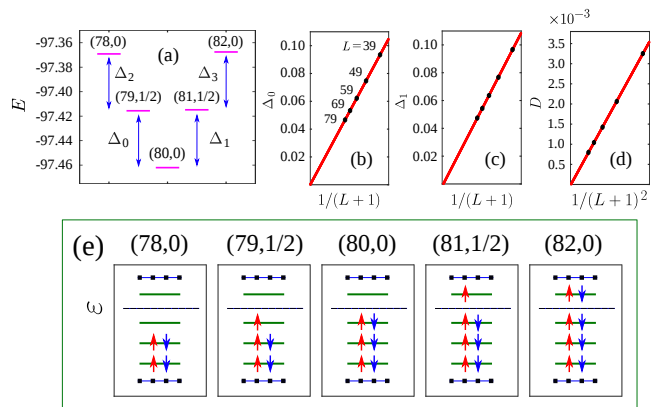


FIG. 2. (a) Energy spectrum of the $L = 79$ system. Each column corresponds to a sector whose quantum numbers are indicated as (N_f, S_z) in the panel. (b)-(d) Scaling relations of three quantities in the energy spectrum. (e) Schematics of the Fermi liquid picture for the energy spectrum.

values of $E(L, N_f, 0)$ with even N_f . For instance, our DMRG results at $L = 79$ and $N_f = 78, 80, 82$ have absolute errors of the 10^{-7} order, so they are almost exact. DMRG calculations also confirm that the half-filled states are the ground states.

The low-lying energy levels of the $L = 79$ system are presented and analyzed in Fig. 2. The differences in energy eigenvalues are characterized by $\Delta_0 = E(L, L, 1/2) - E(L, L + 1, 0)$, $\Delta_1(L) = E(L, L + 2, 1/2) - E(L, L + 1, 0)$, and $D(L) = \Delta_1(L) - \Delta_0(L) = E(L, L + 2, 1/2) - E(L, L, 1/2)$. The finite-size scaling analysis in Fig. 2 (b)-(c) reveals that (i) Δ_0 and Δ_1 go to zero as $1/(L + 1)$, and (ii) $D(L)$ go to zero as $1/(L + 1)^2$. The same L dependence is also observed in $\Delta_2 = E(L, L - 1, 0) - E(L, L + 1, 0)$, $\Delta_3(L) = E(L, L + 3, 0) - E(L, L + 1, 0)$, and $\Delta_3(L) - \Delta_2(L)$. The energy spectrum can be interpreted using the Fermi liquid picture of Nozières as illustrated in Fig. 2 (e): there is a Fermi level at $\varepsilon_0 = 0$, the single-particle energy levels are equally spaced at $\varepsilon_m = \pm \frac{2\pi v_F}{L+1} (m - \frac{1}{2})$ ($m = 1, 2, \dots$ and v_F is the Fermi velocity), the ground state is constructed by filling all the single-particle states below the Fermi level, and the excited states are obtained by adding and/or removing some fermions from the ground state.

The spin-spin correlation function $\Gamma_j = \langle \Psi | \mathbf{S}_0 \cdot \mathbf{S}_j | \Psi \rangle / \langle \Psi | \Psi \rangle$ for the $L = 79$ system is shown in Fig. 3 [37]. As an important signature of the Kondo physics, the decaying behavior of Γ_j has been studied extensively using CFT and numerical methods [49–52]. One generally observes a crossover from $1/r$ decay in the Kondo screening cloud to $1/r^2$ decay outside the cloud. The latter is easy to understand because the system behaves essentially as free fermions once the impurity is completely screened. For our model, the distance between the sites 0 and j is defined as $R_j = \frac{2(L+1)}{\pi} \sin \frac{\theta_j}{2}$ [53]. The log-log plot of $|\Gamma_j|$ versus

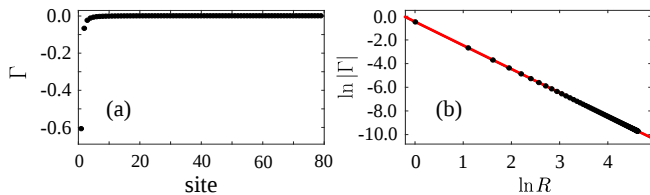


FIG. 3. Spin-spin correlation function Γ of the $L = 79$ system. (a) Γ_j on all sites. (b) Log-log plot of $|\Gamma_j|$ versus $R_j = \frac{2(L+1)}{\pi} \sin \frac{\theta_j}{2}$.

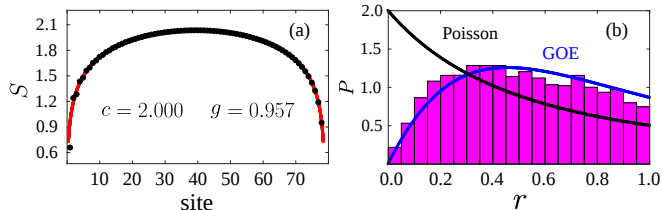


FIG. 4. (a) von Neumann entanglement entropy of the ground state of the $L = 79$, $N_f = 80$, $S_z = 0$ system. The red line is the least square fit using the data points in $10 \leq L_A \leq 70$. (b) Energy level statistics of the $L = 9$ system in the subspace with $N_f = 10$, $S_z = 0$, $\mathbf{S}^2 = 0$. The bars are the probability density of the ratio r_m and the lines are the Poisson and GOE results.

R_j in Fig. 3 (b) has a slope -2.000 with a coefficient of determination higher than 99.99%. This means that the Kondo screening length is extremely short so we can only see the free fermion decay.

The von Neumann entanglement entropy has also been studied. It is defined as $S(L_A) = -\text{Tr}(\rho_A \ln \rho_A)$ with ρ_A being the reduced density matrix for the subsystem $0 \leq j \leq L_A$. It is expected that the Calabrese-Cardy formula

$$S(L_A) = \frac{c}{6} \ln \left[\frac{L}{\pi} \sin \left(\pi \frac{L_A}{L} \right) \right] + g \quad (8)$$

is still applicable outside the Kondo screening cloud [54, 55], where c is the CFT central charge and g is a non-universal number. For the $L = 79$, $N_f = 80$, $S_z = 0$ case, the data points in the range $10 \leq L_A \leq 70$ can be fitted using $c = 2.000$ and $g = 0.957$ as shown in Fig. 4 (a). This is consistent with the fact that the system contains two gapless modes. For the first few sites, there are obvious deviations from the Calabrese-Cardy formula, which should reflect certain aspects of the coupling between the impurity and conduction fermions, but it is unclear how to extract such information.

It is natural to ask if our model is integrable given that a large class of inverse-square models, such as the celebrated Haldane-Shastry model, has been proved to be integrable [56–59]. One diagnostic of integrability is level statistics of the energy spectrum [60, 61]. The eigenvalues E_m are sorted according to the conserved quantum numbers and arranged in ascending order, then the

level spacing $\delta_m = E_{m+1} - E_m$ and the ratio $r_m = \min(\delta_m, \delta_{m+1}) / \max(\delta_m, \delta_{m+1})$ can be obtained. The probability density of r_m have two possible forms: a Poisson distribution with $P(r) = 2/(1+r)^2$ for integrable models and a Gaussian orthogonal ensemble (GOE) with $P(r) = [27(r+r^2)]/[4(1+r+r^2)^{5/2}]$ for non-integrable models. It is quite plausible that our model obeys the GOE distribution as shown in Fig. 4 (b). The expectation value of r_m is 0.511, quite close to the theoretical value 0.536 for GOE. This suggests that our model is not integrable despite having explicit forms for the ground states in all sectors with even N_f .

Conformal field theory formulation — The successful construction of an exactly solvable model for the spin-1/2 Kondo problem with polynomial wave function motivates us to search for similar scenarios in more complicated quantum impurity systems, such as the multichannel and $SU(N)$ Kondo problems. A promising route along this direction manifests itself as soon as we establish a link between the wave function and the associated boundary CFT, which is very similar to the practice of constructing quantum Hall wave functions from edge CFT [35]. The key observation is that the wave function (2) can be represented as a CFT correlator [37]

$$\Psi(\{n_j^\uparrow\}, \{n_j^\downarrow\}) = \langle \mathcal{O}_{\text{bg}} A^{n_0^\uparrow, n_0^\downarrow}(u_0) A^{n_1^\uparrow, n_1^\downarrow}(u_1) \cdots A^{n_L^\uparrow, n_L^\downarrow}(u_L) \rangle \quad (9)$$

with a background charge \mathcal{O}_{bg} controlling the total number of fermions and vertex operators

$$A^{n_j^\uparrow, n_j^\downarrow}(u_j) = \begin{cases} \delta_{n_j, 1} : e^{i \sum_\sigma n_j^\sigma \phi_\sigma(u_j)} : & j = 0 \\ : e^{i \sum_\sigma n_j^\sigma \phi_\sigma(u_j)} : & j = 1, \dots, L \end{cases}, \quad (10)$$

where $\phi_\sigma(u_j)$ is a two-component chiral bosonic field and $: \cdots :$ denotes normal ordering.

This reformulation can be viewed as an infinite-dimensional matrix product state [62] and turns out to be very illuminating in further analysis. If the vertex operators for the impurity site were removed from Eq. (9), the wave function reduces to the ground state of H_0 that realizes the free-fermion CFT with the free boundary condition on the lattice [63–66]. This is perhaps not too surprising, since the vertex operators (10) for conduction fermions all have conformal weight $h = 1/2$ and thus are fermionic fields. However, from the boundary CFT perspective, it is known that the impurity site plays the role of boundary condition changing (BCC) operator as it changes the free boundary condition of conduction fermions to the “Kondo boundary condition” [67]. One may speculate that the vertex operator on the impurity site in Eq. (9) acts as a BCC operator which changes the free boundary condition at one end of the chain to the Kondo boundary condition. Furthermore, the fact that the vertex operator at the impurity site [first line of Eq. (10)] is also a fermionic field with conformal weight

$h = 1/2$ suggests that the Fermi liquid picture holds. The identification of our wave function as a CFT correlator would shed light on how to design other models with CFT inspired wave functions.

Conclusion and discussion — In summary, we have constructed an exactly solvable quantum impurity model with a highly structured ground state and a parent Hamiltonian consists of inverse-square hopping and interaction terms. The low-energy physics of our model is described by a boundary CFT and a particular correlator of this CFT reproduces the wave function. This work establishes a connection between the wave function and boundary CFT in quantum impurity models, which paves the way toward constructing wave functions and exactly solvable models for more complicated systems with SU(N) fermions and/or multiple impurities [68]. For Kondo problems that cannot be solved exactly, we may define ζ^\dagger modes with unknown parameters and use Eq. (3) as variational ansatz. The numerical prospect of optimizing these parameters with respect to some given Hamiltonians is left for future works.

Acknowledgment — We are grateful to Jan von Delft, Biao Huang, Seung-Sup Lee, Frédéric Mila, Germán Sierra, Andreas Weichselbaum, and Guang-Ming Zhang for helpful discussions. This work was supported by the DFG via project A06 (HHT) of SFB 1143 (project-id 247310070), the NSFC under Grant No. 11804107 (YHW), and the startup grant of HUST (YHW).

* hong-hao.tu@tu-dresden.de

† yinghaiwu88@hust.edu.cn

- [1] A. C. Hewson, *The Kondo Problem to Heavy Fermions* (Cambridge University Press, Cambridge, 1997).
- [2] P. Coleman, *Introduction to Many-Body Physics* (Cambridge University Press, Cambridge, 2015).
- [3] D. Goldhaber-Gordon, H. Shtrikman, D. Mahalu, D. Abusch-Magder, U. Meirav, and M. A. Kastner, *Nature* **391**, 156 (1998).
- [4] S. M. Cronenwett, T. H. Oosterkamp, and L. P. Kouwenhoven, *Science* **281**, 540 (1998).
- [5] V. Madhavan, W. Chen, T. Jamneala, M. F. Crommie, and N. S. Wingreen, *Science* **280**, 567 (1998).
- [6] J. Nygård, D. H. Cobden, and P. E. Lindelof, *Nature* **408**, 342 (2000).
- [7] P. Jarillo-Herrero, J. Kong, H. S. van der Zant, C. Dekker, L. P. Kouwenhoven, and S. De Franceschi, *Nature* **434**, 484 (2005).
- [8] Z. Iftikhar, S. Jezouin, A. Anthore, U. Gennser, F. D. Parmentier, A. Cavanna, and F. Pierre, *Nature* **526**, 233 (2015).
- [9] A. J. Keller, L. Peeters, C. P. Moca, I. Weymann, D. Mahalu, V. Umansky, G. Zarnd, and D. Goldhaber-Gordon, *Nature* **526**, 237 (2015).
- [10] Z. Iftikhar, A. Anthore, A. K. Mitchell, F. D. Parmentier, U. Gennser, A. Ouerghi, A. Cavanna, C. Mora, P. Simon, and F. Pierre, *Science* **360**, 1315 (2018).
- [11] B. Béri and N. R. Cooper, *Phys. Rev. Lett.* **109**, 156803 (2012).
- [12] N. Crampe and A. Trombettoni, *Nucl. Phys. B* **871**, 526 (2013).
- [13] A. M. Tsvelik, *Phys. Rev. Lett.* **110**, 147202 (2013).
- [14] A. Altland, B. Béri, R. Egger, and A. M. Tsvelik, *Phys. Rev. Lett.* **113**, 076401 (2014).
- [15] E. Eriksson, C. Mora, A. Zazunov, and R. Egger, *Phys. Rev. Lett.* **113**, 076404 (2014).
- [16] O. Kashuba and C. Timm, *Phys. Rev. Lett.* **114**, 116801 (2015).
- [17] P. W. Anderson, *Phys. Rev.* **124**, 41 (1961).
- [18] J. Kondo, *Prog. Theor. Phys.* **32**, 37 (1964).
- [19] J. R. Schrieffer and P. A. Wolff, *Phys. Rev.* **149**, 491 (1966).
- [20] K. G. Wilson, *Rev. Mod. Phys.* **47**, 773 (1975).
- [21] H. R. Krishna-murthy, J. W. Wilkins, and K. G. Wilson, *Phys. Rev. B* **21**, 1003 (1980).
- [22] R. Bulla, T. A. Costi, and T. Pruschke, *Rev. Mod. Phys.* **80**, 395 (2008).
- [23] P. Nozières, *J. Low Temp. Phys.* **17**, 31 (1974).
- [24] I. Affleck, *Nucl. Phys. B* **336**, 517 (1990).
- [25] I. Affleck and A. W. W. Ludwig, *Nucl. Phys. B* **352**, 849 (1991).
- [26] N. Andrei, *Phys. Rev. Lett.* **45**, 379 (1980).
- [27] P. B. Wiegmann, *JETP Lett* **31**, 364 (1980).
- [28] N. Andrei, K. Furuya, and J. H. Lowenstein, *Rev. Mod. Phys.* **55**, 331 (1983).
- [29] A. M. Tsvelik and P. B. Wiegmann, *Adv. Phys.* **32**, 453 (1983).
- [30] N. Andrei and H. Johannesson, *Phys. Lett. A* **100**, 108 (1984).
- [31] P. Schlottmann, *J. Phys.: Condens. Matter* **3**, 6617 (1991).
- [32] E. S. Sørensen, S. Eggert, and I. Affleck, *J. Phys. A* **26**, 6757 (1993).
- [33] H. Frahm and A. A. Zvyagin, *J. Phys.: Condens. Matter* **9**, 9939 (1997).
- [34] Y. Wang, J. Dai, Z. Hu, and F.-C. Pu, *Phys. Rev. Lett.* **79**, 1901 (1997).
- [35] G. Moore and N. Read, *Nucl. Phys. B* **360**, 362 (1991).
- [36] $\cos^0 \theta_j$ is undefined at $\theta_j = \pi/2$, but we take it to be 1 to simplify our notation.
- [37] See the Appendices for more details on the wave function, the parent Hamiltonian, and the spin-spin correlation function.
- [38] P. W. Anderson, P. A. Lee, M. Randeria, T. M. Rice, N. Trivedi, and F. C. Zhang, *J. Phys.: Condens. Matter* **16**, R755 (2004).
- [39] B. Edegger, V. N. Muthukumar, and C. Gros, *Adv. Phys.* **56**, 927 (2007).
- [40] R. B. Laughlin, [arXiv:cond-mat/0209269](https://arxiv.org/abs/cond-mat/0209269) (2002).
- [41] M. Kollar, [arXiv:cond-mat/0308513](https://arxiv.org/abs/cond-mat/0308513) (2003).
- [42] K. Yosida, *Phys. Rev.* **147**, 223 (1966).
- [43] J. Kondo, *Phys. Rev.* **161**, 598 (1967).
- [44] B. Sutherland, *Beautiful models: 70 years of exactly solved quantum many-body problems* (World Scientific, Singapore, 2004).
- [45] S. R. White, *Phys. Rev. Lett.* **69**, 2863 (1992).
- [46] U. Schollwöck, *Ann. Phys.* **326**, 96 (2011).
- [47] C. Hubig, I. P. McCulloch, U. Schollwöck, and F. A. Wolf, *Phys. Rev. B* **91**, 155115 (2015).
- [48] C. Hubig, I. P. McCulloch, and U. Schollwöck, *Phys. Rev. B* **95**, 035129 (2017).

- [49] V. Barzykin and I. Affleck, *Phys. Rev. B* **57**, 432 (1998).
- [50] T. Hand, J. Kroha, and H. Monien, *Phys. Rev. Lett.* **97**, 136604 (2006).
- [51] L. Borda, *Phys. Rev. B* **75**, 041307 (2007).
- [52] A. Holzner, I. P. McCulloch, U. Schollwöck, J. von Delft, and F. Heidrich-Meisner, *Phys. Rev. B* **80**, 205114 (2009).
- [53] This is the case if we change the radius to $\frac{L+1}{\pi}$ in Fig. 1 (a) and use the chord distance between two sites. It ensures that $R_j \approx j$ when $j \ll L$. The linear coordinates u_j are rescaled but the wave function is only modified in a trivial way.
- [54] P. Calabrese and J. Cardy, *J. Stat. Mech.* **2004**, P06002 (2004).
- [55] I. Affleck, N. Laflorencie, and E. S. Sørensen, *J. Phys. A: Math. Theor.* **42**, 504009 (2009).
- [56] F. D. M. Haldane, *Phys. Rev. Lett.* **60**, 635 (1988).
- [57] B. S. Shastry, *Phys. Rev. Lett.* **60**, 639 (1988).
- [58] F. D. M. Haldane, Z. N. C. Ha, J. C. Talstra, D. Bernard, and V. Pasquier, *Phys. Rev. Lett.* **69**, 2021 (1992).
- [59] D. Bernard, M. Gaudin, F. D. M. Haldane, and V. Pasquier, *J. Phys. A* **26**, 5219 (1993).
- [60] D. Poilblanc, T. Ziman, J. Bellissard, F. Mila, and G. Montambaux, *Europhys. Lett.* **22**, 537 (1993).
- [61] Y. Y. Atas, E. Bogomolny, O. Giraud, and G. Roux, *Phys. Rev. Lett.* **110**, 084101 (2013).
- [62] J. I. Cirac and G. Sierra, *Phys. Rev. B* **81**, 104431 (2010).
- [63] H.-H. Tu and G. Sierra, *Phys. Rev. B* **92**, 041119 (2015).
- [64] B. Basu-Mallick, F. Finkel, and A. González-López, *Phys. Rev. B* **93**, 155154 (2016).
- [65] J.-M. Stéphan and F. Pollmann, *Phys. Rev. B* **95**, 035119 (2017).
- [66] A. Hackenbroich and H.-H. Tu, *Nucl. Phys. B* **916**, 1 (2017).
- [67] I. Affleck and A. W. W. Ludwig, *J. Phys. A* **27**, 5375 (1994).
- [68] Y.-H. Wu and H.-H. Tu, [arXiv:1906.03464](https://arxiv.org/abs/1906.03464) (2019).

APPENDIX A: WAVE FUNCTION

This section provides more details about the properties of the ground-state wave function

$$\Psi(\{n_j^\uparrow\}, \{n_j^\downarrow\}) = \delta_{n_0=1} \delta_{\sum_j n_j^\uparrow = \sum_j n_j^\downarrow = M} \prod_{\sigma=\uparrow,\downarrow} \prod_{0 \leq j < k \leq L} (u_j - u_k)^{n_j^\sigma n_k^\sigma}. \quad (\text{A1})$$

A1: Gutzwiller projected Fermi sea

We first prove Eq. (3) of the main text. To begin with, we can rewrite the ground state as

$$|\Psi\rangle = \sum_{\{n_j^\uparrow\}, \{n_j^\downarrow\}} \Psi(\{n_j^\uparrow\}, \{n_j^\downarrow\}) (c_{0,\uparrow}^\dagger)^{n_0^\uparrow} \cdots (c_{L,\uparrow}^\dagger)^{n_L^\uparrow} (c_{0,\downarrow}^\dagger)^{n_0^\downarrow} \cdots (c_{L,\downarrow}^\dagger)^{n_L^\downarrow} |0\rangle = P_0^G |\tilde{\Psi}\rangle. \quad (\text{A2})$$

The Gutzwiller projector P_j^G enforces the single-occupancy constraint $\delta_{n_0=1}$ on the impurity site $j = 0$ and the state $|\tilde{\Psi}\rangle$ is

$$\begin{aligned} & \sum_{\{n_j^\uparrow\}, \{n_j^\downarrow\}} \delta_{\sum_j n_j^\uparrow = \sum_j n_j^\downarrow = M} \left[\prod_{\sigma=\uparrow,\downarrow} \prod_{0 \leq j < k \leq L} (u_j - u_k)^{n_j^\sigma n_k^\sigma} \right] (c_{0,\uparrow}^\dagger)^{n_0^\uparrow} \cdots (c_{L,\uparrow}^\dagger)^{n_L^\uparrow} (c_{0,\downarrow}^\dagger)^{n_0^\downarrow} \cdots (c_{L,\downarrow}^\dagger)^{n_L^\downarrow} |0\rangle \\ &= \sum_{x_1 < \cdots < x_M} \sum_{y_1 < \cdots < y_M} \left[\prod_{1 \leq j < k \leq M} (u_{x_j} - u_{x_k}) \prod_{1 \leq j < k \leq M} (u_{y_j} - u_{y_k}) \right] c_{x_1,\uparrow}^\dagger \cdots c_{x_M,\uparrow}^\dagger c_{y_1,\downarrow}^\dagger \cdots c_{y_M,\downarrow}^\dagger |0\rangle, \end{aligned} \quad (\text{A3})$$

where $\{x_1, \dots, x_M\}$ and $\{y_1, \dots, y_M\}$ are the lattice sites occupied by spin-up and spin-down fermions, respectively. The Jastrow factor $\prod_{1 \leq j < k \leq M} (u_{x_j} - u_{x_k})$ can be converted to a Vandermonde determinant

$$(-1)^{\frac{1}{2}M(M-1)} \det \begin{pmatrix} 1 & 1 & \cdots & 1 \\ u_{x_1} & u_{x_2} & \cdots & u_{x_M} \\ \vdots & \vdots & \ddots & \vdots \\ u_{x_1}^{M-1} & u_{x_2}^{M-1} & \cdots & u_{x_M}^{M-1} \end{pmatrix}, \quad (\text{A4})$$

so one can see that

$$\begin{aligned} |\tilde{\Psi}\rangle &\propto \sum_{\{x_i\}, \{y_i\}} \det \begin{pmatrix} 1 & 1 & \cdots & 1 \\ u_{x_1} & u_{x_2} & \cdots & u_{x_M} \\ \vdots & \vdots & \ddots & \vdots \\ u_{x_1}^{M-1} & u_{x_2}^{M-1} & \cdots & u_{x_M}^{M-1} \end{pmatrix} \det \begin{pmatrix} 1 & 1 & \cdots & 1 \\ u_{y_1} & u_{y_2} & \cdots & u_{y_M} \\ \vdots & \vdots & \ddots & \vdots \\ u_{y_1}^{M-1} & u_{y_2}^{M-1} & \cdots & u_{y_M}^{M-1} \end{pmatrix} c_{x_1,\uparrow}^\dagger \cdots c_{x_M,\uparrow}^\dagger c_{y_1,\downarrow}^\dagger \cdots c_{y_M,\downarrow}^\dagger |0\rangle \\ &\propto \prod_{m=0}^{M-1} \prod_{\sigma=\uparrow,\downarrow} \eta_{m,\sigma}^\dagger |0\rangle, \end{aligned} \quad (\text{A5})$$

with $\eta_{m,\sigma} = \sum_{j=0}^L u_j^m c_{j,\sigma}$. The substitution of Eq. (A5) into Eq. (A2) completes the proof.

The Gutzwiller projection can be performed explicitly to facilitate our construction of the parent Hamiltonian. For this purpose, we use the linear combinations of the η modes to define some ζ modes

$$\zeta_{0,\sigma} = \eta_{0,\sigma} - c_{0,\sigma} = \sum_{j=1}^L c_j, \quad \zeta_{m,\sigma} = \eta_{m-1,\sigma} - \eta_{m,\sigma} = \sum_{j=1}^L \cos^{m-1} \theta_j (1 - \cos \theta_j) c_{j,\sigma} \quad \text{for } m \geq 1. \quad (\text{A6})$$

For odd L , it is possible to have $\theta_j = \pi/2$ such that $\cos^{m-1} \theta_j$ is undefined at $m = 1$. For these cases, we define

$\cos^0 \theta_j \equiv 1$ to simplify our notation. The ground state is transformed to

$$\begin{aligned}
|\Psi\rangle &= P_0^G \eta_{0,\uparrow}^\dagger \eta_{0,\downarrow}^\dagger \prod_{m=1}^{M-1} \prod_{\sigma=\uparrow,\downarrow} \eta_{m,\sigma}^\dagger |0\rangle \\
&= P_0^G \left(c_{0,\uparrow}^\dagger + \zeta_{0,\uparrow}^\dagger \right) \left(c_{0,\downarrow}^\dagger + \zeta_{0,\downarrow}^\dagger \right) \prod_{m=1}^{M-1} \prod_{\sigma=\uparrow,\downarrow} \zeta_{m,\sigma}^\dagger |0\rangle \\
&= \left(c_{0,\uparrow}^\dagger \zeta_{0,\downarrow}^\dagger - c_{0,\downarrow}^\dagger \zeta_{0,\uparrow}^\dagger \right) \prod_{m=1}^{M-1} \prod_{\sigma=\uparrow,\downarrow} \zeta_{m,\sigma}^\dagger |0\rangle.
\end{aligned} \tag{A7}$$

A3: Conformal field theory formulation

This subsection aims to prove Eq. (10) of the main text. The chiral bosonic field for spin-up fermions is defined by $\phi_\uparrow(u) = \phi_0^\dagger - i\pi_0^\dagger \ln u + i \sum_{n \neq 0} \frac{1}{n} a_n^\dagger u^{-n}$, where ϕ_0^\dagger , π_0^\dagger , and a_n^\dagger are operators satisfying the following commutation relations: $[\phi_0^\dagger, \pi_0^\dagger] = i$ and $[a_n^\dagger, a_m^\dagger] = n\delta_{n+m,0}$. Furthermore, π_0^\dagger and $a_{n>0}^\dagger$ annihilate the vacuum $|0\rangle$, i.e., $\pi_0^\dagger |0\rangle = a_{n>0}^\dagger |0\rangle = 0$. The corresponding chiral vertex operator for spin-up fermion is given by

$$: \exp [i\phi_\uparrow(u)] := \exp \left(i\phi_0^\dagger + \sum_{n=1}^{\infty} \frac{1}{n} a_{-n}^\dagger u^n \right) \exp \left(\pi_0^\dagger \ln u - \sum_{n=1}^{\infty} \frac{1}{n} a_n^\dagger u^{-n} \right). \tag{A8}$$

For odd L , $\theta_{j=(L+1)/2} = \pi/2$ and, for this site, the corresponding vertex operator only includes the zero-mode part $\exp(i\phi_0^\dagger)$. For spin-down fermions, the expressions of the chiral bosonic field and vertex operators are similar, with the spin index replaced by \downarrow .

The product of chiral vertex operators is obtained by normal ordering of operators

$$\begin{aligned}
&: \exp [i\phi_\uparrow(u_{x_1})] : \cdots : \exp [i\phi_\uparrow(u_{x_M})] : \\
&= \exp \left(iM\phi_0^\dagger + \sum_{m=1}^M \sum_{n=1}^{\infty} \frac{1}{n} a_{-n}^\dagger u_{x_m}^n \right) \exp \left[\pi_0^\dagger \ln(u_{x_1} \cdots u_{x_M}) - \sum_{m=1}^M \sum_{n=1}^{\infty} \frac{1}{n} a_n^\dagger u_{x_m}^{-n} \right] \\
&\times \prod_{1 \leq i < j \leq M} (u_{x_i} - u_{x_j}).
\end{aligned} \tag{A9}$$

The electron vertex operators can be neutralized using a background charge operator

$$O_{bg}^\dagger = \exp \left(-iM\phi_0^\dagger \right), \tag{A10}$$

so that the following chiral correlator (expectation value in the CFT vacuum $|0\rangle$) yields the Jastrow product for spin-up fermions

$$\langle O_{bg}^\dagger : \exp [i\phi_\uparrow(u_{x_1})] : \cdots : \exp [i\phi_\uparrow(u_{x_M})] : \rangle = \prod_{1 \leq i < j \leq M} (u_{x_i} - u_{x_j}). \tag{A11}$$

For the wave function with both spin-up and spin-down fermions being present, the background charge should be defined as $O_{bg} = O_{bg}^\dagger O_{bg}^\dagger$.

APPENDIX B: PARENT HAMILTONIAN

This section provides details about how to act the parent Hamiltonian on the ground state. The target state is a superposition of two parts in which the spin on the $j = 0$ site points up and down, respectively. When acted upon by an operator, the result can still be written like this. To simplify subsequent analysis, we focus on the spin-up part. The spin-down part can be analyzed in the same way. For notational ease, we denote $\prod_{m=1}^{M-1} \prod_{\sigma=\uparrow,\downarrow} \zeta_{m,\sigma}^\dagger |0\rangle$ as $|\text{PFS}\rangle$ (PFS stands for partial Fermi sea).

B1: The Kondo term

The Kondo term is

$$H_K = \mathbf{S}_0 \cdot \Lambda_K = \frac{1}{2} S_0^+ \Lambda_K^- + \frac{1}{2} S_0^- \Lambda_K^+ + S_0^z \Lambda_K^z \quad (\text{A12})$$

with

$$\Lambda_K = \sum_{j=1}^L \frac{1 + \cos \theta_j}{1 - \cos \theta_j} \mathbf{S}_j = \sum_{j=1}^L \cot^2 \frac{\theta_j}{2} \mathbf{S}_j. \quad (\text{A13})$$

As for usual spin operators, one can also define Λ_K^+ , Λ_K^- , and Λ_K^z . Their commutators with the ζ modes are

$$\begin{aligned} [\Lambda_K^-, \zeta_{0,\uparrow}^\dagger] &= \sum_{j=1}^L \frac{1 + \cos \theta_j}{1 - \cos \theta_j} c_{j,\downarrow}^\dagger \equiv O_{K,\downarrow}, \quad [\Lambda_K^-, \zeta_{m,\uparrow}^\dagger] = 2\zeta_{0,\downarrow}^\dagger - 2 \sum_{\alpha=1}^{m-1} \zeta_{\alpha,\downarrow}^\dagger - \zeta_{m,\downarrow}^\dagger \quad \text{for } m > 0, \\ [\Lambda_K^-, \zeta_{m,\downarrow}^\dagger] &= 0 \quad \text{for } m \geq 0, \\ [\Lambda_K^z, \zeta_{0,\uparrow}^\dagger] &= \frac{1}{2} \sum_{j=1}^L \frac{1 + \cos \theta_j}{1 - \cos \theta_j} c_{j,\uparrow}^\dagger \equiv \frac{1}{2} O_{K,\uparrow}, \quad [\Lambda_K^z, \zeta_{m,\uparrow}^\dagger] = \zeta_{0,\uparrow}^\dagger - \sum_{\alpha=1}^{m-1} \zeta_{\alpha,\uparrow}^\dagger - \frac{1}{2} \zeta_{m,\uparrow}^\dagger \quad \text{for } m > 0, \\ [\Lambda_K^z, \zeta_{0,\downarrow}^\dagger] &= -\frac{1}{2} \sum_{j=1}^L \frac{1 + \cos \theta_j}{1 - \cos \theta_j} c_{j,\downarrow}^\dagger = -\frac{1}{2} O_{K,\downarrow}, \quad [\Lambda_K^z, \zeta_{m,\downarrow}^\dagger] = -\zeta_{0,\downarrow}^\dagger + \sum_{\alpha=1}^{m-1} \zeta_{\alpha,\downarrow}^\dagger + \frac{1}{2} \zeta_{m,\downarrow}^\dagger \quad \text{for } m > 0. \end{aligned} \quad (\text{A14})$$

The action of H_K on $|\Psi\rangle$ gives $|\Psi_K^\uparrow\rangle + |\Psi_K^\downarrow\rangle$ with

$$|\Psi_K^\uparrow\rangle = c_{0,\uparrow}^\dagger \left(-\frac{1}{2} \Lambda_K^- \zeta_{0,\uparrow}^\dagger + \frac{1}{2} \Lambda_K^z \zeta_{0,\downarrow}^\dagger \right) |\text{PFS}\rangle = c_{0,\uparrow}^\dagger \left(-\frac{3}{4} O_{K,\downarrow} - \frac{1}{2} \zeta_{0,\uparrow}^\dagger \Lambda_K^- + \frac{1}{2} \zeta_{0,\downarrow}^\dagger \Lambda_K^z \right) |\text{PFS}\rangle. \quad (\text{A15})$$

The commutators listed above can be used to show that

$$\begin{aligned} \zeta_{0,\uparrow}^\dagger \Lambda_K^- |\text{PFS}\rangle &= 2 \sum_{m=1}^{M-1} \zeta_{0,\uparrow}^\dagger \zeta_{0,\downarrow}^\dagger \left[\prod_{\alpha=1}^{m-1} \zeta_{\alpha,\uparrow}^\dagger \zeta_{\alpha,\downarrow}^\dagger \right] \zeta_{m,\downarrow}^\dagger \left[\prod_{\alpha=m+1}^{M-1} \zeta_{\alpha,\uparrow}^\dagger \zeta_{\alpha,\downarrow}^\dagger \right] |0\rangle, \\ \zeta_{0,\downarrow}^\dagger \Lambda_K^z |\text{PFS}\rangle &= - \sum_{m=1}^{M-1} \zeta_{0,\uparrow}^\dagger \zeta_{0,\downarrow}^\dagger \left[\prod_{\alpha=1}^{m-1} \zeta_{\alpha,\uparrow}^\dagger \zeta_{\alpha,\downarrow}^\dagger \right] \zeta_{m,\downarrow}^\dagger \left[\prod_{\alpha=m+1}^{M-1} \zeta_{\alpha,\uparrow}^\dagger \zeta_{\alpha,\downarrow}^\dagger \right] |0\rangle. \end{aligned} \quad (\text{A16})$$

The terms in Eq. (A15) are unwanted in the sense that they do not appear in the target state. However, the result is not bad because the unwanted terms in Eq. (A16) are highly structured. The $O_{K,\downarrow}$ term is somewhat special, so our next step would be to eliminate it.

B2: The site-dependent potential term

The site-dependent potential term is

$$H_P = \frac{3}{4} \sum_{j=1}^L \sum_{\sigma=\uparrow,\downarrow} \frac{1 + \cos \theta_j}{1 - \cos \theta_j} c_{j,\sigma}^\dagger c_{j,\sigma} = \frac{3}{4} \sum_{j=1}^L \sum_{\sigma=\uparrow,\downarrow} \cot^2 \frac{\theta_j}{2} c_{j,\sigma}^\dagger c_{j,\sigma}. \quad (\text{A17})$$

Its commutators with the ζ modes are

$$[H_P, \zeta_{0,\sigma}^\dagger] = \frac{3}{4} \sum_{j=1}^L \frac{1 + \cos \theta_j}{1 - \cos \theta_j} c_{j,\sigma}^\dagger = \frac{3}{4} O_{K,\sigma}, \quad [H_P, \zeta_{m,\sigma}^\dagger] = \frac{3}{2} \zeta_{0,\sigma}^\dagger - \frac{3}{2} \sum_{\alpha=1}^{m-1} \zeta_{\alpha,\sigma}^\dagger - \frac{3}{4} \zeta_{m,\sigma}^\dagger \quad \text{for } m > 0. \quad (\text{A18})$$

The action of H_P on $|\Psi\rangle$ gives $|\Psi_P^\uparrow\rangle + |\Psi_P^\downarrow\rangle$ with

$$|\Psi_P^\uparrow\rangle = c_{0,\uparrow}^\dagger H_P \zeta_{0,\downarrow}^\dagger |\text{PFS}\rangle = c_{0,\uparrow}^\dagger \left(\frac{3}{4} O_{K,\downarrow} + \zeta_{0,\downarrow}^\dagger H_P \right) |\text{PFS}\rangle. \quad (\text{A19})$$

The commutators listed above can be used to show that

$$\zeta_{0,\downarrow}^\dagger H_P |\text{PFS}\rangle = -\frac{3}{2} \sum_{m=1}^{M-1} \zeta_{0,\uparrow}^\dagger \zeta_{0,\downarrow}^\dagger \left[\prod_{\alpha=1}^{m-1} \zeta_{\alpha,\uparrow}^\dagger \zeta_{\alpha,\downarrow}^\dagger \right] \zeta_{m,\downarrow}^\dagger \left[\prod_{\alpha=m+1}^{M-1} \zeta_{\alpha,\uparrow}^\dagger \zeta_{\alpha,\downarrow}^\dagger \right] |0\rangle - \frac{3}{2} (M-1) \zeta_{0,\downarrow}^\dagger |\text{PFS}\rangle. \quad (\text{A20})$$

At this point, one can see why this choice of H_P is promising: the $O_{K,\downarrow}$ terms in Eqs. (A15) and (A19) cancel each other; the unwanted terms in Eq. (A20) have the same form as those in Eq. (A16). It is obvious that $|\Psi_K^\dagger\rangle + |\Psi_P^\dagger\rangle$ is

$$c_{0,\uparrow}^\dagger \left\{ -3 \sum_{m=1}^{M-1} \zeta_{0,\uparrow}^\dagger \zeta_{0,\downarrow}^\dagger \left[\prod_{\alpha=1}^{m-1} \zeta_{\alpha,\uparrow}^\dagger \zeta_{\alpha,\downarrow}^\dagger \right] \zeta_{m,\downarrow}^\dagger \left[\prod_{\alpha=m+1}^{M-1} \zeta_{\alpha,\uparrow}^\dagger \zeta_{\alpha,\downarrow}^\dagger \right] |0\rangle \right\} - \frac{3}{2} (M-1) c_{0,\uparrow}^\dagger \zeta_{0,\downarrow}^\dagger |\text{PFS}\rangle, \quad (\text{A21})$$

where the first term represents particle-hole excitations on top of the Fermi sea. In order to find a parent Hamiltonian, these particle-hole excitations should be canceled by contributions from $H_0 |\text{PFS}\rangle$.

B3: The hopping term

The hopping term is designed as

$$H_0 = \sum_{q=0}^{L-1} \sum_{\sigma=\uparrow,\downarrow} 3q^2 d_{q,\sigma}^\dagger d_{q,\sigma}, \quad (\text{A22})$$

where

$$d_{q,\sigma} = \begin{cases} \frac{1}{\sqrt{L}} \sum_{j=1}^L c_{j,\sigma} & \text{for } q=0 \\ \sqrt{\frac{2}{L}} \sum_{j=1}^L \cos(q\theta_j) c_{j,\sigma} & \text{for } 1 \leq q \leq L-1 \end{cases}. \quad (\text{A23})$$

The angles are chosen to be $\theta_j = \frac{\pi}{L}(j - \frac{1}{2})$ to make sure that the fermionic modes $d_{q,\sigma}$ form an orthonormal and complete single-particle basis. This can be verified using the discrete orthogonality property of the Chebyshev polynomials.

Let us prove that H_0 has an inverse-square form in the original fermion basis. It is obvious that

$$\begin{aligned} H_0 &= \sum_{q=1}^{L-1} \sum_{j,k} \frac{6}{L} q^2 \cos(q\theta_j) \cos(q\theta_k) c_{j,\sigma}^\dagger c_{k,\sigma} \\ &= \sum_{j=1}^L \sum_{q=1}^{L-1} \frac{3}{L} q^2 [1 + \cos(2q\theta_j)] c_{j,\sigma}^\dagger c_{j,\sigma} + \sum_{j,k=1; j \neq k}^L \sum_{q=1}^{L-1} \frac{3}{L} q^2 [\cos(q\theta_j - q\theta_k) + \cos(q\theta_j + q\theta_k)] c_{j,\sigma}^\dagger c_{k,\sigma} \\ &= \sum_{j=1}^L \sum_{q=1}^{L-1} \frac{3}{L} q^2 \left\{ 1 + \cos \left[\frac{q\pi}{L} (2j-1) \right] \right\} c_{j,\sigma}^\dagger c_{j,\sigma} \\ &\quad + \sum_{j,k=1; j \neq k}^L \sum_{q=1}^{L-1} \frac{3}{L} q^2 \left\{ \cos \left[\frac{q\pi}{L} (j-k) \right] + \cos \left[\frac{q\pi}{L} (j+k+1) \right] \right\} c_{j,\sigma}^\dagger c_{k,\sigma}. \end{aligned} \quad (\text{A24})$$

For an integer $X \in [0, 2L)$, we have the summation identity

$$\sum_{q=1}^{L-1} q^2 \cos \left(\frac{q\pi}{L} X \right) = \begin{cases} \frac{(-1)^X}{2} L \left[\frac{1}{\sin^2 \left(\frac{\pi X}{2L} \right)} - 1 \right] & X \neq 0 \\ \frac{1}{6} L(L-1)(2L-1) & X = 0 \end{cases}. \quad (\text{A25})$$

This helps us to show that

$$\begin{aligned} H_0 &= \sum_{j,k=1; j \neq k}^L (-1)^{j-k} \left(\frac{6}{|z_j - z_k|^2} - \frac{6}{|z_j - z_k^*|^2} \right) c_{j,\sigma}^\dagger c_{k,\sigma} \\ &\quad + \sum_{j=1}^L \left[L^2 + \frac{1}{2} - \frac{3}{2 \sin^2 \theta_j} \right] c_{j,\sigma}^\dagger c_{j,\sigma}, \end{aligned} \quad (\text{A26})$$

where $z_j = \exp(i\theta_j)$ and $z_j^* = \exp(-i\theta_j)$ are the complex coordinates of the site j and its mirror image, respectively.

To compute the results of acting H_0 on $|\Psi\rangle$, we need to know commutators of the $[H_0, \zeta_m^\dagger]$ type. This requires linear transformations between the two sets of single-particle orbitals defined by (the spin index σ is suppressed below for simplicity)

$$\zeta_m^\dagger = \sum_{q=0}^{L-1} W_{mq} d_q^\dagger \quad d_q^\dagger = \sum_{m=0}^{L-1} (W^{-1})_{qm} \zeta_m^\dagger, \quad (\text{A27})$$

One can see that

$$\begin{aligned} [H_0, \zeta_m^\dagger] &= \sum_{q, q'=0}^{L-1} 3q^2 W_{mq'} [d_q^\dagger d_q, d_{q'}^\dagger] = \sum_{q=0}^{L-1} 3q^2 W_{mq} d_q^\dagger \\ &= \sum_{q=0}^{L-1} \sum_{m'=0}^{L-1} 3q^2 W_{mq} (W^{-1})_{qm'} \zeta_{m'}^\dagger = \sum_{m'=0}^{L-1} A_{mm'} \zeta_{m'}^\dagger \end{aligned}$$

with

$$A_{mm'} = \sum_{q=0}^{L-1} 3q^2 W_{mq} (W^{-1})_{qm'}. \quad (\text{A28})$$

For the $m = 0$ case, we have $[H_0, \zeta_0^\dagger] = 0$ because d_0^\dagger is a zero mode of H_0 and $\zeta_0^\dagger = \sqrt{L}d_0^\dagger$. This helps us to prove that $H_0|\Psi\rangle = |\Psi_0^\uparrow\rangle + |\Psi_0^\downarrow\rangle$ with

$$\begin{aligned} |\Psi_0^\uparrow\rangle &= c_{0,\uparrow}^\dagger H_0 \zeta_{0,\downarrow}^\dagger |\text{PFS}\rangle = c_{0,\uparrow}^\dagger \zeta_{0,\downarrow}^\dagger H_0 |\text{PFS}\rangle \\ &= c_{0,\uparrow}^\dagger \left\{ -\zeta_{0,\uparrow}^\dagger \zeta_{0,\downarrow}^\dagger \sum_{m=1}^{M-1} \left[\prod_{\alpha=1}^{m-1} \zeta_{\alpha,\uparrow}^\dagger \zeta_{\alpha,\downarrow}^\dagger \right] A_{m0} \zeta_{m,\downarrow}^\dagger \left[\prod_{\alpha=m+1}^{M-1} \zeta_{\alpha,\uparrow}^\dagger \zeta_{\alpha,\downarrow}^\dagger \right] |0\rangle + 2\zeta_{0,\downarrow}^\dagger \sum_{m=1}^{M-1} A_{mm} |\text{PFS}\rangle \right\}, \quad (\text{A29}) \end{aligned}$$

so the diagonal entries A_{mm} and the first column A_{m0} of the matrix $A_{mm'}$ are sufficient for our purpose.

Let us consider the transformation matrix from d_q^\dagger to ζ_m^\dagger . The $m = 0$ case is simple since $\zeta_0^\dagger = \sum_{j=1}^L c_j^\dagger = \sqrt{L}d_0^\dagger$. For $m \geq 1$, we have

$$\begin{aligned} \zeta_m^\dagger &= \sum_{j=1}^L \cos^{m-1} \theta_j (1 - \cos \theta_j) c_j^\dagger \\ &= \sum_{j=1}^L \left[\left(\frac{e^{i\theta_j} + e^{-i\theta_j}}{2} \right)^{m-1} - \left(\frac{e^{i\theta_j} + e^{-i\theta_j}}{2} \right)^m \right] c_j^\dagger \\ &= \sum_{j=1}^L \frac{c_j^\dagger}{2^m} \times \\ &\quad \begin{cases} 2 \sum_{\alpha=-\frac{m-1}{2}}^{\frac{m-1}{2}} \binom{m-1}{\frac{m-1}{2} + \alpha} e^{i[(\frac{m-1}{2} + \alpha) - (\frac{m-1}{2} - \alpha)]\theta_j} - \sum_{\alpha=-\frac{m+1}{2}}^{\frac{m+1}{2}} \binom{m}{\frac{m-1}{2} + \alpha} e^{i[(\frac{m-1}{2} + \alpha) - (\frac{m+1}{2} - \alpha)]\theta_j} & \text{odd } m \geq 1 \\ 2 \sum_{\alpha=-\frac{m}{2}+1}^{\frac{m}{2}} \binom{m-1}{\frac{m}{2} - 1 + \alpha} e^{i[(\frac{m}{2} - 1 + \alpha) - (\frac{m}{2} - \alpha)]\theta_j} - \sum_{\alpha=-\frac{m}{2}}^{\frac{m}{2}} \binom{m}{\frac{m}{2} + \alpha} e^{i[(\frac{m}{2} + \alpha) - (\frac{m}{2} - \alpha)]\theta_j} & \text{even } m \geq 2 \end{cases} \\ &= \sum_{j=1}^L \frac{c_j^\dagger}{2^m} \begin{cases} 2 \binom{m-1}{\frac{m-1}{2}} + 4 \sum_{\alpha=1}^{\frac{m-1}{2}} \binom{m-1}{\frac{m-1}{2} + \alpha} \cos(2\alpha\theta_j) - 2 \sum_{\alpha=1}^{\frac{m+1}{2}} \binom{m}{\frac{m-1}{2} + \alpha} \cos(2\alpha - 1)\theta_j & \text{odd } m \geq 1 \\ 4 \sum_{\alpha=1}^{\frac{m}{2}} \binom{m-1}{\frac{m}{2} - 1 + \alpha} \cos(2\alpha - 1)\theta_j - \binom{m}{\frac{m}{2}} - 2 \sum_{\alpha=1}^{\frac{m}{2}} \binom{m}{\frac{m}{2} + \alpha} \cos(2\alpha\theta_j) & \text{even } m \geq 2 \end{cases} \\ &= \sqrt{\frac{L}{2}} \frac{1}{2^m} \begin{cases} 2\sqrt{2} \binom{m-1}{\frac{m-1}{2}} d_0^\dagger + 4 \sum_{\alpha=1}^{\frac{m-1}{2}} \binom{m-1}{\frac{m-1}{2} + \alpha} d_{2\alpha}^\dagger - 2 \sum_{\alpha=1}^{\frac{m+1}{2}} \binom{m}{\frac{m-1}{2} + \alpha} d_{2\alpha-1}^\dagger & \text{odd } m \geq 1 \\ 4 \sum_{\alpha=1}^{\frac{m}{2}} \binom{m-1}{\frac{m}{2} - 1 + \alpha} d_{2\alpha-1}^\dagger - \sqrt{2} \binom{m}{\frac{m}{2}} d_0^\dagger - 2 \sum_{\alpha=1}^{\frac{m}{2}} \binom{m}{\frac{m}{2} + \alpha} d_{2\alpha}^\dagger & \text{even } m \geq 2 \end{cases}. \quad (\text{A30}) \end{aligned}$$

Its derivatives are

$$(m-1)(x+x^{-1})^{m-2}(1-x^{-2}) = \sum_{\alpha=1}^{\frac{m-1}{2}} \binom{m-1}{\frac{m-1}{2} + \alpha} 2\alpha (x^{2\alpha-1} - x^{-2\alpha-1}) \quad (\text{A45})$$

and

$$\begin{aligned} & (m-1)(m-2)(x+x^{-1})^{m-3}(1-x^{-2})^2 + (m-1)(x+x^{-1})^{m-2} \frac{2}{x^3} \\ &= \sum_{\alpha=1}^{\frac{m-1}{2}} \binom{m-1}{\frac{m-1}{2} + \alpha} 2\alpha [(2\alpha-1)x^{2\alpha-2} + (2\alpha+1)x^{-2\alpha-2}]. \end{aligned} \quad (\text{A46})$$

If x is chosen to be 1 in Eq. (A46), we obtain

$$(m-1)2^{m-1} = \sum_{\alpha=1}^{\frac{m-1}{2}} \binom{m-1}{\frac{m-1}{2} + \alpha} 8\alpha^2. \quad (\text{A47})$$

For odd m , we study

$$\begin{aligned} (x+x^{-1})^m &= \sum_{\alpha=-\frac{m-1}{2}}^{\frac{m+1}{2}} \binom{m}{\frac{m-1}{2} + \alpha} x^{\frac{m-1}{2} + \alpha} x^{-(\frac{m+1}{2} - \alpha)} \\ &= \sum_{\alpha=-\frac{m-1}{2}}^{\frac{m+1}{2}} \binom{m}{\frac{m-1}{2} + \alpha} x^{2\alpha-1} = \sum_{\alpha=1}^{\frac{m+1}{2}} \binom{m}{\frac{m-1}{2} + \alpha} (x^{2\alpha-1} + x^{-2\alpha+1}). \end{aligned}$$

Its derivatives are

$$m(x+x^{-1})^{m-1}(1-x^{-2}) = \sum_{\alpha=1}^{\frac{m+1}{2}} \binom{m}{\frac{m-1}{2} + \alpha} [(2\alpha-1)x^{2\alpha-2} - (2\alpha-1)x^{-2\alpha}], \quad (\text{A48})$$

and

$$\begin{aligned} & m(m-1)(x+x^{-1})^{m-2}(1-x^{-2})^2 + m(x+x^{-1})^{m-1} \frac{2}{x^3} \\ &= \sum_{\alpha=1}^{\frac{m+1}{2}} \binom{m}{\frac{m-1}{2} + \alpha} [(2\alpha-1)(2\alpha-2)x^{2\alpha-3} + (2\alpha-1)2\alpha x^{-2\alpha-1}]. \end{aligned} \quad (\text{A49})$$

If x is chosen to be 1 in Eq. (A49), we obtain

$$m2^{m-1} = \sum_{\alpha=1}^{\frac{m+1}{2}} \binom{m}{\frac{m-1}{2} + \alpha} (2\alpha-1)^2. \quad (\text{A50})$$

The sums with even m can be obtained from previous ones. In Eq. (A47), replacing $m-1$ with m yields

$$m2^m = \sum_{\alpha=1}^{\frac{m}{2}} \binom{m}{\frac{m}{2} + \alpha} 8\alpha^2. \quad (\text{A51})$$

In Eq. (A50), replacing $m+1$ with m yields

$$(m-1)2^{m-2} = \sum_{\alpha=1}^{\frac{m}{2}} \binom{m-1}{\frac{m}{2} - 1 + \alpha} (2\alpha-1)^2. \quad (\text{A52})$$

APPENDIX C: SPIN-SPIN CORRELATION FUNCTION

This section provides more details about how to compute the spin-spin correlation function of the ground state. To begin with, we compute the overlap of two generic free fermion states. For a set of fermionic operators c_j^\dagger and c_j satisfying the anticommutation relations, we define two sets of operators α_a^\dagger and β_b^\dagger

$$\alpha_a = \sum_j U_{aj} c_j, \quad \beta_b = \sum_j V_{bj} c_j, \quad (\text{A53})$$

where U_{aj} and V_{bj} are two matrices that may not be isometry. It is easy to see that

$$\langle 0 | \alpha_a \beta_b^\dagger | 0 \rangle = \sum_{jk} U_{aj} V_{bk}^* \langle 0 | c_j c_k^\dagger | 0 \rangle = \sum_j U_{aj} V_{bj}^* = \sum_j [UV^\dagger]_{ab} = G_{ab} \quad (\text{A54})$$

with $G = UV^\dagger$. The overlap between $\alpha_1^\dagger \alpha_2^\dagger \cdots \alpha_M^\dagger | 0 \rangle$ and $\beta_1^\dagger \beta_2^\dagger \cdots \beta_M^\dagger | 0 \rangle$ is found to be

$$\begin{aligned} & \langle 0 | \alpha_M \cdots \alpha_2 \alpha_1 \beta_1^\dagger \beta_2^\dagger \cdots \beta_M | 0 \rangle \\ &= \langle 0 | \alpha_1 \beta_1^\dagger | 0 \rangle \langle 0 | \alpha_2 \beta_2^\dagger | 0 \rangle \cdots \langle 0 | \alpha_M \beta_M^\dagger | 0 \rangle + \text{all possible permutations with signs} \\ &= G_{11} G_{22} \cdots G_{MM} + \text{all possible permutations with signs} \\ &= \det G \end{aligned} \quad (\text{A55})$$

using Eq. (A54) and Wick's theorem.

The numerator of the spin-spin correlation function can be simplified using the SU(2) spin symmetry as

$$\langle \Psi | \mathbf{S}_0 \cdot \mathbf{S}_j | \Psi \rangle = \langle \Psi | S_0^x S_j^x | \Psi \rangle = \frac{3}{2} (\langle \Psi | S_0^x S_j^x | \Psi \rangle + \langle \Psi | S_0^y S_j^y | \Psi \rangle) = \frac{3}{2} \langle \Psi | S_0^+ S_j^- | \Psi \rangle \quad (\text{A56})$$

with

$$\begin{aligned} \langle \Psi | S_0^+ S_j^- | \Psi \rangle &= \langle 0 | \prod_{m=M-1}^{j-1} \prod_{\sigma=\downarrow, \uparrow} \zeta_{m,\sigma} \zeta_{0,\uparrow} c_{j,\uparrow} c_{j,\downarrow}^\dagger \zeta_{0,\uparrow}^\dagger \prod_{m=1}^{M-1} \prod_{\sigma=\uparrow, \downarrow} \zeta_{m,\sigma}^\dagger | 0 \rangle \\ &= -\langle 0 | \prod_{m=M-1}^{j-1} \zeta_{m,\uparrow} c_{j,\uparrow} \zeta_{0,\uparrow}^\dagger \prod_{m=1}^{M-1} \zeta_{m,\uparrow}^\dagger | 0 \rangle \cdot \langle 0 | \prod_{m=M-1} \zeta_{m,\downarrow} \zeta_{0,\downarrow} c_{j,\downarrow}^\dagger \prod_{m=1}^{M-1} \zeta_{m,\downarrow}^\dagger | 0 \rangle, \end{aligned} \quad (\text{A57})$$

where $\prod_{m=M-1}^{j-1} \prod_{\sigma=\downarrow, \uparrow} \zeta_{m,\sigma}$ denotes reversed order of products. The denominator of the spin-spin correlation function is the unnormalized overlap

$$\begin{aligned} \langle \Psi | \Psi \rangle &= \langle 0 | \prod_{m=M-1}^{j-1} \zeta_{m,\uparrow} \prod_{m=1}^{M-1} \zeta_{m,\uparrow}^\dagger | 0 \rangle \cdot \langle 0 | \prod_{m=M-1} \zeta_{m,\downarrow} \zeta_{0,\downarrow} \zeta_{0,\downarrow}^\dagger \prod_{m=1}^{M-1} \zeta_{m,\downarrow}^\dagger | 0 \rangle \\ &+ \langle 0 | \prod_{m=M-1}^{j-1} \zeta_{m,\uparrow} \zeta_{0,\uparrow} \zeta_{0,\uparrow}^\dagger \prod_{m=1}^{M-1} \zeta_{m,\uparrow}^\dagger | 0 \rangle \cdot \langle 0 | \prod_{m=M-1} \zeta_{m,\downarrow} \prod_{m=1}^{M-1} \zeta_{m,\downarrow}^\dagger | 0 \rangle. \end{aligned} \quad (\text{A58})$$

Both of them can be computed using Eq. (A55).